OncoTargets and Therapy

Dovepress
Taylor & Francis Group

Open Access Full Text Article

ORIGINAL RESEARCH

Integrating Bulk and Single-Cell RNA Sequencing Data Reveals the Prognostic Significance of HOXC9-Related Immune Gene Signatures in Hepatocellular Carcinoma

Yong Zhang[1,*], Hengliang Sun[2,*], Weibo Bo[1], Zhongwu An[1], Jing Li[3]

[1]Department of Clinical Laboratory, Lianyungang Municipal Oriental Hospital, Lianyungang, Jiangsu, 222042, People's Republic of China; [2]Department of Clinical Laboratory, Hai'an Hospital of Traditional Chinese Medicine, Hai'an, Jiangsu, 226600, People's Republic of China; [3]Department of Respiratory and Critical Care Medicine, Lianyungang Municipal Oriental Hospital, Lianyungang, Jiangsu, 222042, People's Republic of China

*These authors contributed equally to this work

Correspondence: Jing Li, Department of Respiratory and Critical Care Medicine, Lianyungang Municipal Oriental Hospital, No. 57 Zhonghua West Road, Lianyun District, Lianyungang, Jiangsu Province, 222042, People's Republic of China, Email 15261379272@163.com

Objective: This study aims to integrate bulk and single-cell RNA sequencing data to construct a risk score model based on HOXC9-related immune genes (HRIGs) and evaluate its prognostic value in hepatocellular carcinoma (HCC).

Materials and Methods: RNA sequencing data and clinical information of HCC were obtained from TCGA and GEO databases. HRIGs were identified and a risk score model was constructed using LASSO-Cox regression analysis. The association between the risk score and tumor microenvironment was analyzed using CIBERSORT and ESTIMATE algorithms. Single-cell RNA sequencing (scRNA-seq) data were used to assess cell type distribution. Cell experiments were conducted to verify the effects of HOXC9 knockdown on HCC cell proliferation and invasion.

Results: HOXC9 is highly expressed in HCC and associated with poor prognosis ($p=0.031$). The risk score model based on four HRIGs (EGLN3, IMPDH1, LPCAT1, and MARCKSL1) showed good prognostic discrimination in both TCGA and GEO cohorts, with significantly lower overall survival in the high-risk group ($p<0.0001$). The high-risk group exhibited higher immune scores and increased immune cell infiltration, as well as elevated immune checkpoint expression. scRNA-seq revealed increased hepatocytes and fibroblasts but decreased T/NK cells in HCC tissues. HOXC9 knockdown significantly inhibited HCC cell proliferation and invasion.

Conclusion: HOXC9 is overexpressed in HCC and correlates with poor prognosis. The HRIG-based risk score model effectively evaluates the prognosis and immune response in HCC patients, providing new insights for risk assessment and immunotherapy prediction.

Keywords: hepatocellular carcinoma, HOXC9, risk score model, immunotherapy, tumor microenvironment

Introduction

Hepatocellular carcinoma (HCC) ranks sixth in incidence and third in mortality rates across various cancer types worldwide, thus imposing a substantial healthcare burden on the population.[1–5] Although HCC treatments like hepatectomy, liver transplantation, interventional therapy, targeted therapy, and immunotherapy have made significant progress in precision and personalized therapy, the 5-year survival rate for patients has stagnated at approximately 18%.[5–9] A significant amount of research has confirmed that the early symptoms of HCC are atypical, and the lack of early diagnostic methods is the main reason why the disease often progresses to an advanced stage, leading to poor prognosis.[9,10]

In recent years, immunotherapy, both as monotherapy and in combination, has played an increasingly important role in treating advanced HCC.[11] The combination of Atezolizumab and Bevacizumab for HCC patients undergoing

Received: 1 December 2024
Accepted: 23 March 2025
Published: 29 March 2025

transcatheter arterial chemoembolization (TACE) has significantly improved progression-free survival (PFS), with manageable safety.[12–15] In addition, Durvalumab combined with Tremelimumab treatment has a significant survival benefit compared with Sorafenib, but the median overall survival (OS) is close to Durvalumab monotherapy, and the survival benefit is limited.[14] However, increasing evidence has shown that severe immune-related adverse events (irAEs), such as hypertransaminasemia, can not only limit the benefits patients receive from immunotherapy but also pose a life-threatening risk.[16,17] Therefore, monitoring irAEs in patients with advanced HCC undergoing immunotherapy is of significant clinical importance. Guven et al found that patients with lower albumin levels had a significantly increased risk of death, suggesting that albumin may be a prognostic biomarker for patients with advanced cancer receiving immunotherapy.[18]

The homeobox genes were first detected in *Drosophila melanogaster*, where they are referred to as homeotic complex (HOM-C) genes and are categorized within the homeobox gene family.[19–21] In mammals, homeobox genes are segregated into two subfamilies. The initial subfamily—the A–P type—is closely situated on chromosomes and exhibits an anterior–posterior (A–P) expression pattern, encompassing the HOX genes. The second subfamily comprises homeobox genes that are not the A–P type and are not clustered but distributed across different chromosomes.[22] These genes are grouped into specific clusters, such as empty spiracles (EMX), paired-box (PAX), muscle segment homeobox (MSH), and orthodenticle-related (OTX) families based on sequence similarities. The complex network of homeobox genes in various organisms emphasizes the evolutionary conservation and functional importance of these genetic components. Studies suggest that HOXC9 is a pivotal transcription factor in embryonic development, contributing to essential biological processes like cell growth, differentiation, and apoptosis. Abnormalities in the expression of HOXC9 have been related to different cancer types, demonstrating both tumorigenic and tumor-suppressive features. Moreover, HOXC9 expression level is closely associated with the clinical features and OS of patients with cancer.

The present study mainly aimed to explore the prognostic gene HOXC9 and investigate how it relates to immune infiltration levels and pathological conditions in individuals with HCC. A risk-scoring model for HRIGs was developed and verified, resulting in the construction of a nomogram. Furthermore, this study also examined the correlations among risk score, TME, and immune infiltration. This study provides novel insights for risk assessment and immune response prediction in patients with HCC.

Methods

Data Acquisition

The RNA-seq data and the corresponding clinicopathological data of the HCC project were obtained from The Cancer Genome Atlas (TCGA) website. The transcripts per million (TPM) expression levels for all genes were collected and aggregated across the entire set of samples. Subsequently, the GSE14520 matrix file was procured from the Gene Expression Omnibus (GEO) database. The cohort from TCGA comprised 374 hCC samples and 50 normal samples. By integrating RNA-seq data and clinical data, a total of 365 hCC patient data were obtained. The GEO cohort (GSE14520) was composed of 242 hCC samples and 246 normal samples. A Kaplan-Meier (KM) curve was generated to assess the prognostic significance of HOXC9 in patients with HCC. This study chose the single-cell RNA-seq (scRNA-seq) dataset GSE149614 from the GEO database. This dataset comprises 10 samples of primary tumors, 2 samples of portal vein tumor thrombi, 1 sample of metastatic lymph node, and 8 samples of non-tumor liver. Following the analysis of the scRNA-seq data of 10 hCC samples and 8 normal samples, the R package “Seurat” was used to address the batch effects among these samples. Cells with a gene count ranging from 200 to 7,500 and a mitochondrial gene proportion < 15% were included in the analysis, whereas cells identified as low quality were excluded from the dataset. Ultimately, a total of 61,706 cells were retained for further investigation.

Relationship Between HOXC9 Expression, TME, and Immune Infiltration

The study investigated the correlation between HOXC9 and immune cells by determining the infiltration scores of 22 immune cell types in HCC tissues through the cell-type identification by estimating relative subsets of RNA transcripts (CIBERSORT) algorithm.[23,24] The Spearman method was used to evaluate the association between HOXC9 expression

and the above 22 immune cell types. Additionally, the immune cell infiltration levels in groups with varying levels of HOXC9 expression were also analyzed. The estimation of stromal and immune cells in malignant tumor tissues using expression data (ESTIMATE) algorithm was used to determine the StromalScore, ImmuneScore, and ESTIMATEScore for individual tumor samples.[25] Subsequently, a detailed examination was conducted to investigate the potential correlations between HOXC9 expression and these scores.

Construction and Validation of an HRIG Risk Score Model

According to the screening criteria of $p < 0.05$ and correlation coefficient (cor) > 0.25, a total of 743 genes related to HOXC9 and 3,190 genes related to immune score were identified. Subsequently, 171 hub genes were determined. Following this, the genes were subjected to the least absolute shrinkage and selection operator (LASSO)-Cox regression analysis. Ultimately, a set of four genes (EGLN3, IMPDH1, LPCAT1, and MARCKSL1) were selected to construct the prognostic risk model. The following formula was utilized to calculate the risk score:

Risk score = Coefficient (Coefi) EGLN3 × EGLN3 mRNA expression + Coefi IMPDH1 × IMPDH1 mRNA expression + Coefi LPCAT1 × LPCAT1 mRNA expression + Coefi MARCKSL1 × MARCKSL1 mRNA expression.

The z-score function was applied to compute the z-score for each sample, whereby samples with a z-score ≥ 0 were designated as the high-risk group, whereas those with a z-score < 0 were classified as the low-risk group. Subsequently, KM curves were analyzed to compare the survival difference between the high-risk and low-risk groups. The R package "timeROC" was used to evaluate the predictive ability of the prognostic risk signature by analyzing the receiver operating characteristic (ROC) curves for survival rates at 1, 3, and 5 years.

Relationship Between the HRIG Model and Tumor Immunity

The CIBERSORT and microenvironment cell population-counter (MCP-counter) methods were used to explore the variation in immune cell infiltrations between the low- and high-risk groups.[26] Additionally, the differences in immune checkpoint expression between individuals classified as high-risk and low-risk were also examined. The IMvigor210 dataset comprised transcriptomic and clinical information derived from patients diagnosed with bladder cancer (BLCA) who underwent anti-programmed death-ligand 1 (anti-PD-L1) therapy. The importance of the HRIG signatures in predicting the efficacy of immune checkpoint inhibitors (ICIs) in the IMvigor210 cohort.

Development and Verification of a Nomogram Scoring Model

A predictive nomogram was developed using the R package "rms", incorporating risk score, age, gender, T stage, and pathological stage. Each patient's overall score was determined by summing up the individual scores associated with each variable. The calibration curves confirmed the nomogram to be reliable and accurate in predicting 1-, 3-, and 5-year OS.

Cell Culture

The HUH7 and SKHEP1 cell lines were acquired from the Cell Bank of the Chinese Academy of Sciences in Shanghai, China. HUH7 and SKHEP1 cells were cultured in Dulbecco's modified Eagle's medium (DMEM) consisting of 10% fetal bovine serum (FBS) and 1% penicillin/streptomycin, which were then incubated at 37°C with 5% CO_2.

Cell Proliferative Capacity Detection

Cell viability and colony formation assays were conducted to assess the proliferative capacity of HCC cell lines following HOXC9 knockdown. The cell counting kit-8 (CCK8) was utilized to monitor cell viability at designated intervals. In the colony formation test, cells transfected with control and small interfering-HOXC9 (si-HOXC9) were grown in six-well plates, and the colonies were stained with crystal violet after two weeks of incubation.

Cell Invasive Capacity Detection

Diluted Matrigel was placed in the upper chamber of the transwell and incubated at 37°C for 2 hours. After that, it was hydrated with 100 μL of serum-free 1640 medium for 30 minutes. The upper chamber of a transwell plate was seeded

with a total of 20,000 lung adenocarcinoma (LUAD) cells. After incubating for 2 days at 37°C and 5% CO_2, the cells on the membrane surface were immobilized using 0.4% paraformaldehyde and stained with 0.1% crystal violet dye for 20 minutes. Then, the cells were rinsed with phosphate-buffered saline (PBS), and randomly selected, examined, and captured using a light microscope.

Statistical Analysis

The *t*-test and Wilcoxon test were employed for differential expression analysis. The prognostic importance of HOXC9 expression in HCC was assessed utilizing univariate and multivariate Cox regression models and KM curves. A p-value < 0.05 was considered statistically significant.

Results

Correlation of HOXC9 Expression with Prognosis and Immune Infiltration in HCC

Pan-cancer analysis disclosed that HOXC9 is upregulated in various malignant tumors, such as HCC (Figure 1A). KM curves revealed a notable association between increased HOXC9 levels and poor prognosis in patients with HCC ($p = 0.031$) (Figure 1B). HOXC9 expression demonstrated a significant positive relationship with regulatory T (Treg) cells (Figure 1C). The group with high HOXC9 expression showed a significant decrease in M1 macrophages and monocytes compared to the group with low expression (Figure 1D). Furthermore, we investigated the associations between HOXC9 expression levels and various clinicopathological characteristics, including TNM stage, pathologic stage, tumor status, gender, age, histologic grade, AFP levels, and Child-Pugh grade (Supplementary Table 1).

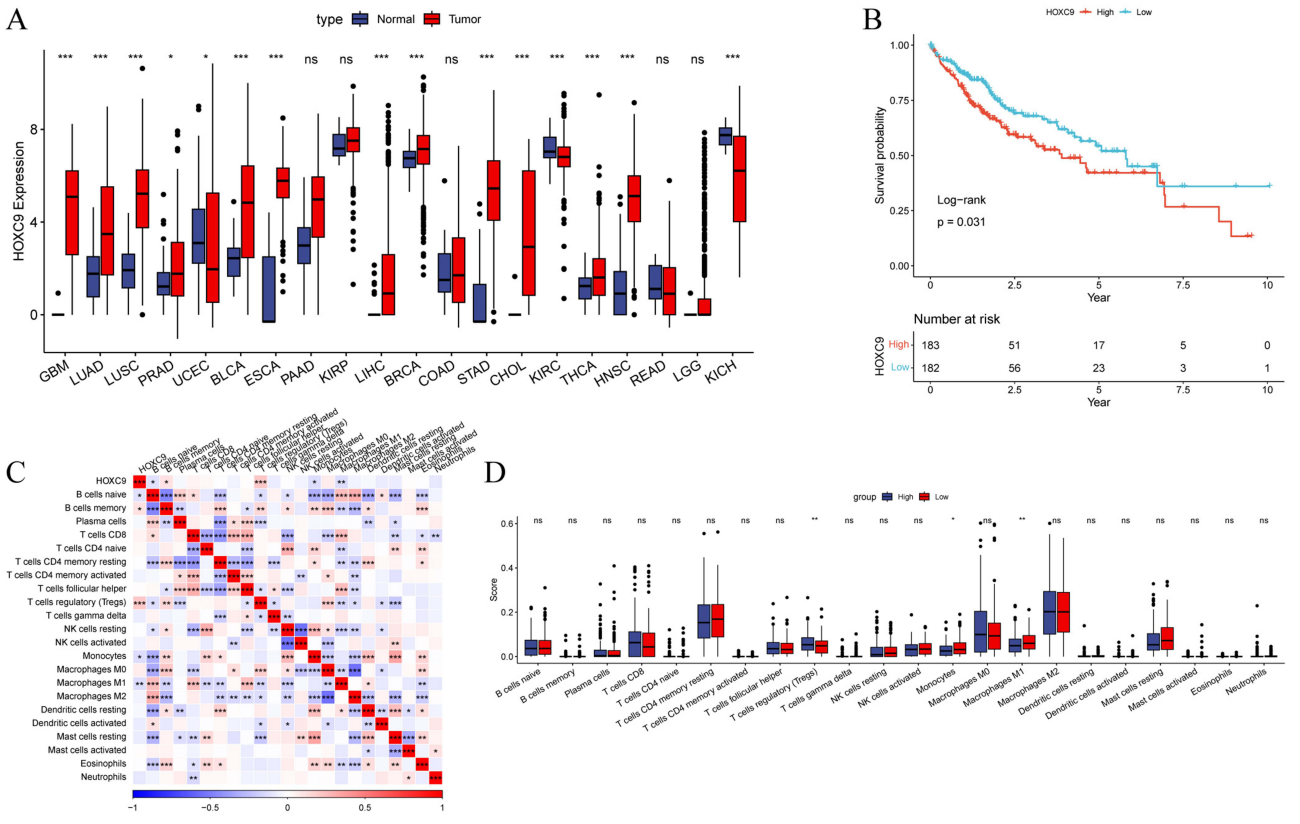

Figure 1 Expression levels of HOXC9 in HCC. (**A**) Human HOXC9 expression levels in different cancer types from TCGA database. (**B**) KM curves of OS for high- and low-HOXC9 expression subpopulations. (**C**) Correlation analysis between HOXC9 gene expression and immune cell infiltration. (**D**) Box plot of 22 immune cells based on CIBERSORT between the high- and low-HOXC9 expression groups in TCGA database. *p < 0.05, **p < 0.01, ***p < 0.001, ns-not statistically significant.

 https://doi.org/10.2147/OTT.S509625

Construction of an HRIG Risk Score Model

A risk-scoring system was created by conducting LASSO-Cox analyses on 171 hRIGs (Figure 2A and B). The HCC samples were categorized into high- and low-risk groups using Z-score values, with the KM curve being utilized to evaluate the differences in survival outcomes. The findings suggest that the patients with high risk demonstrated reduced OS rates in TCGA ($p < 0.0001$) and the GSE14520 cohort ($p = 0.01$) (Figure 2C and D). Within TCGA cohort, the risk-scoring model yielded an area under the curve (AUC) of 0.69, 0.69, and 0.68 for 1-, 3-, and 5-year survival rates, respectively, as shown in Figure 2E. Within the *D* group, this model yielded AUC values of 0.67, 0.67, and 0.6 for 1-, 3-, and 5-year survival rates, respectively, as shown in Figure 2F. Moreover, we generated box plots to illustrate the differential expression of the four HRIGs (EGLN3, IMPDH1, LPCAT1, and MARCKSL1) between liver cancer tissues and adjacent non-tumor tissues using data from the TCGA database (Supplementary Figure 1).

Linking the Risk Model to TME, Immune Cells, and Immune Checkpoints

The CIBERSORT algorithm was employed to evaluate variations in immune cell infiltration among high- and low-risk categories (Figure 3A). The findings showed increased levels of Treg cells and M0 macrophages in the high-risk category. Furthermore, the MCPcounter algorithm indicated elevated levels of fibroblasts and monocytic lineage in the high-risk group (Figure 3B). Figure 3C shows that the high-risk group had higher StromalScore, ImmuneScore, and ESTIMATEScore compared to the low-risk group. Additionally, there was an increased immune checkpoint expression in the high-risk category (Figure 3D).

Immunotherapy Response Prediction

Immunotherapy holds immense potential in anticancer treatments, significantly prolonging the OS and improving the quality of life for patients. Evaluating the relationship between risk models and immunotherapy can offer novel insights into immunotherapy in HCC. The variations in immune response between high-risk and low-risk groups were evaluated using

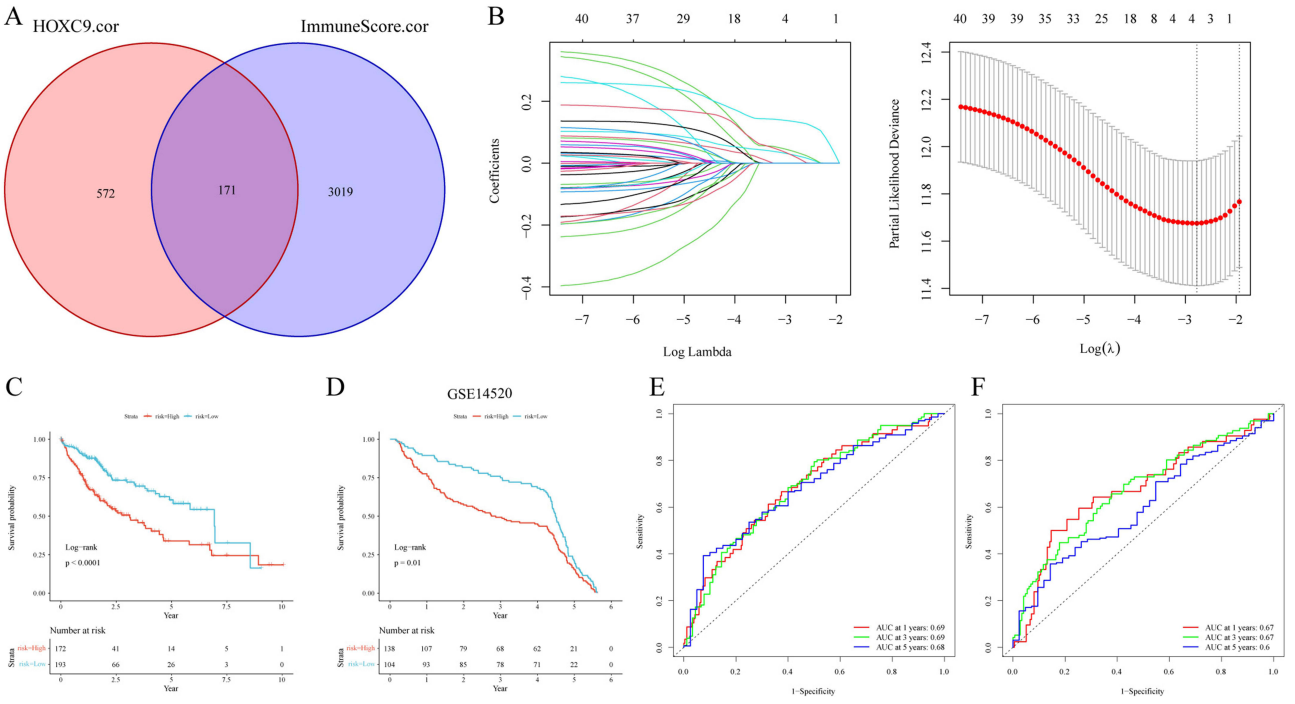

Figure 2 Construction of an HRIG-based risk score model. (**A**) Venn diagram identifying the 169 hRIGs shared by 743 hOXC9-related genes and 3,190 ImmuneScore-related genes. (**B**) LASSO regression analysis of HRIGs. (**C**) Survival analysis of patients in TCGA cohort using HRIG-based risk score model. (**D**) Survival analysis of patients in the GSE14520 cohort based on HRIG-based risk score model. (**E**) Time-dependent ROC curve of HRIG-based risk score model in TCGA dataset. (**F**) Time-dependent ROC curve of HRIG-based risk score model in the GSE14520 dataset.

https://doi.org/10.2147/OTT.S509625

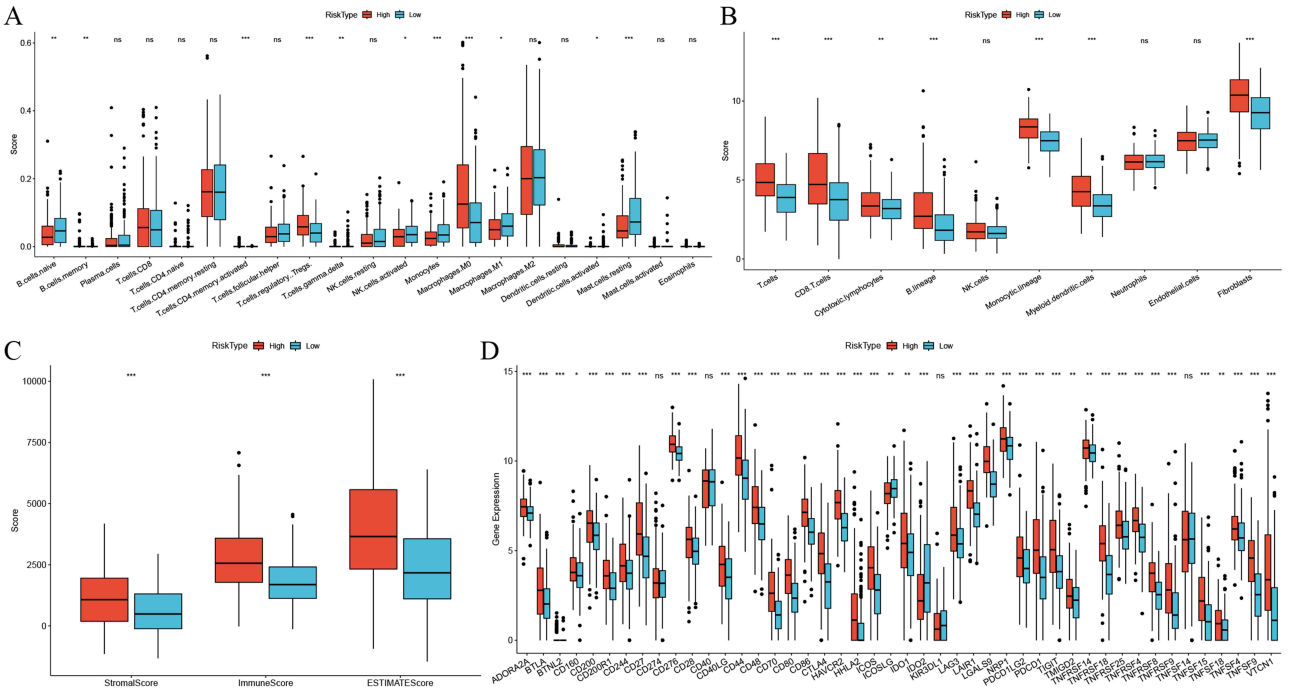

Figure 3 Relationship between HRIG-based risk score model and tumor immunity. (**A**) Differences in immune cell score between two HRIG groups with high and low HRIG signatures (calculated using CIBERSORT). (**B**) Differences in immune cell infiltration between two HRIG groups with high and low HRIG signatures (calculated using MCPcounter). (**C**) Differences in ESTIMATEScore, StromalScore, and ImmuneScore between low- and high-risk groups. (**D**) Differences between the immune checkpoints and two HRIG groups. *p < 0.05, **p < 0.01, ***p < 0.001, ns-not statistically significant.

the IMvigor210 dataset. The findings indicated a lower proportion of immune responses in the high-risk group and a higher proportion of patients in advanced stages, with the chi-squared test results showing significance (Figure 4A and B). KM curves also indicated that individuals classified as high-risk had a reduced OS time (Figure 4C). As shown in Figure 4D, the risk scores for the complete response/partial response (CR/PR) group were notably lower compared to the stable disease/progressive disease (SD/PD) group. Furthermore, patients in advanced stages had notably elevated risk scores compared to those in the early stages (Figure 4E).

Establishment of a Reliable Nomogram for Predicting HCC Prognosis

Univariate and multivariate regression analyses were utilized to evaluate the possibility of HRIG signatures as an independent risk factor. Univariate analysis indicated that T stage, pathological stage, and risk score could serve as independent risk factors, whereas multivariate analysis demonstrated that only risk score could function as an independent risk factor (hazard ratio (HR) = 2.302) (Figure 5A and B). A nomogram was generated to evaluate the potential of risk score and pathological stage in predicting the survival period of patients with HCC. The nomogram accurately forecasted the survival rates of patients at 1, 3, and 5 years according to the calibration curves (Figure 5C and D).

ScRNA-Seq

scRNA-seq offers unparalleled resolution and detail compared to bulk RNA sequencing, enabling the identification of distinct cell types and subtypes, analysis of cell type-specific gene expression patterns, and assessment of immune infiltration. These capabilities are essential for unraveling the cellular complexity of tissues and advancing our understanding of disease mechanisms and therapeutic targets. In the present study, after preprocessing the GSE149614 dataset, scRNA-seq data from HCC and adjacent healthy tissues were merged and subjected to uniform manifold approximation

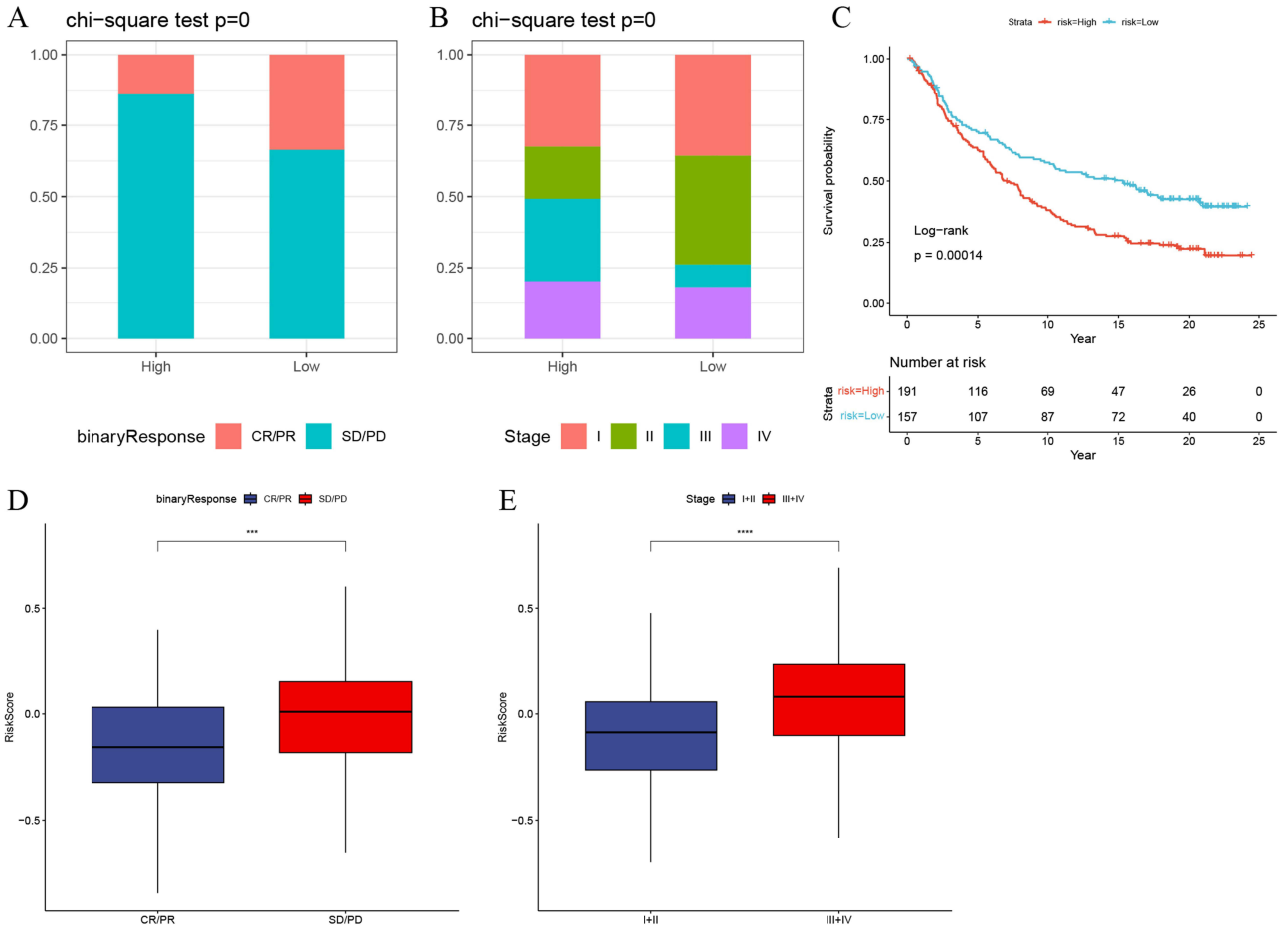

Figure 4 Prediction of immunotherapy efficacy by the risk model. (**A**) The proportion of patients with BLCA in the IMvigor210 low- and high-risk subgroups who responded to anti-PD-L1 therapy. (**B**) Distribution of pathological stages between risk score groups in the IMvigor210 cohort. (**C**) KM curve of IMvigor210 (anti-PD-L1 BLCA) in the low and high-risk groups. (**D**) Risk score differences in immunotherapy responses in the IMvigor210 cohort. (**E**) Risk score differences in pathological stages in the IMvigor210 cohort. ***p < 0.001, ****p < 0.0001, ns-not statistically significant.

and projection (UMAP) non-linear dimension reduction. Based on previous research, six major cell types were identified, including T/NK cells, myeloid cells, endothelial cells, hepatocytes, fibroblasts, and B cells (Figure 6A). The study further evaluated the proportion of these cell types in HCC and healthy tissues, revealing that hepatocytes and fibroblasts were notably increased, while T/NK cells were significantly reduced in HCC tissues compared to normal tissues. Additionally, HOXC9 expression was specifically detected in fibroblasts and hepatocytes within HCC tissues (Figure 6B and C).

Inhibition of HCC Cell Viability, Colony Formation, and Invasion Following HOXC9 Knockdown

Specific siRNAs targeting HOXC9 were utilized to reduce the expression levels of HOXC9 in HCC cells (Supplementary Figure 2). The results from CCK8 and colony formation assays indicated that the decrease in HOXC9 levels suppressed the proliferation of HUH7 and SKHEP1 cells (Figure 7A and B). Additionally, the transwell test showed that blocking HOXC9 reduced the invasive abilities of HCC cells (Figure 7C). Consequently, downregulating HOXC9 could potentially hinder the malignant phenotype of HCC cells.

https://doi.org/10.2147/OTT.S509625

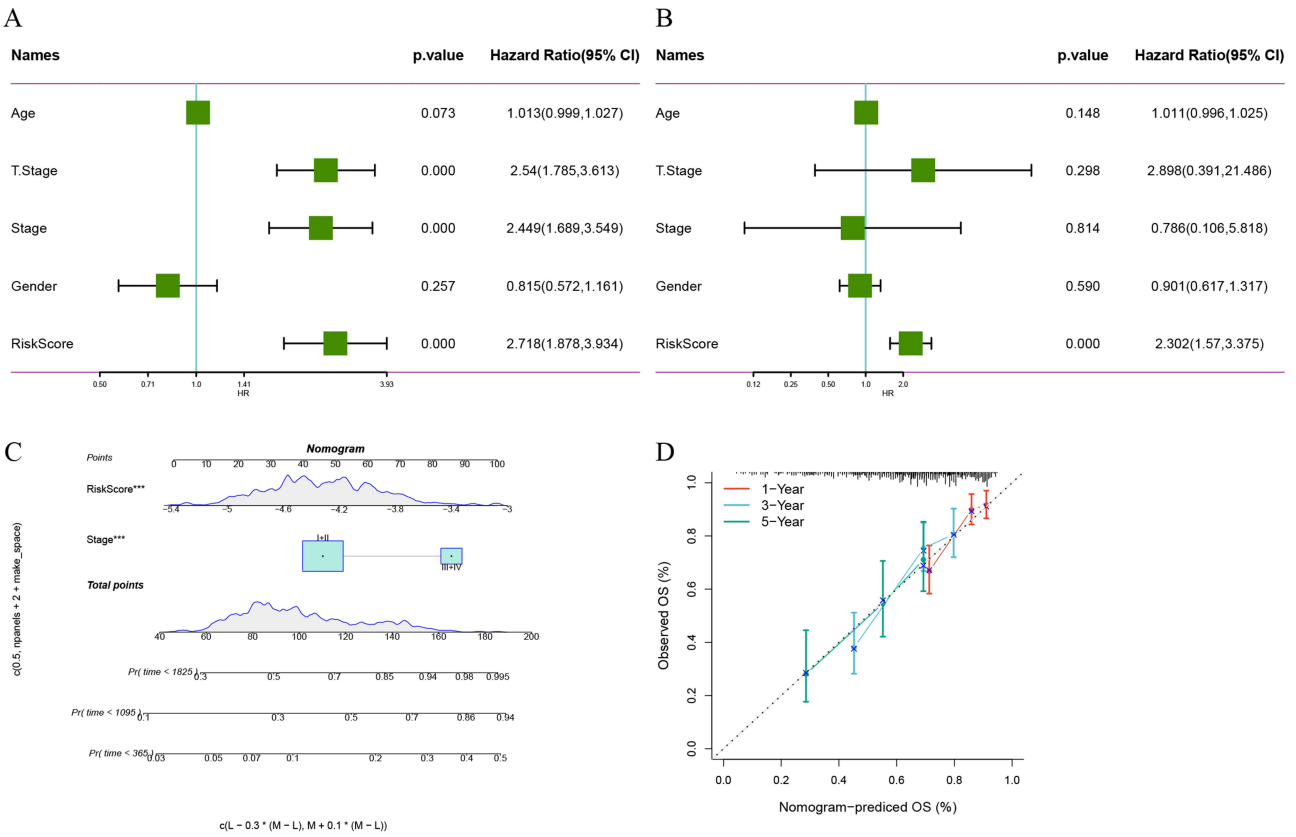

Figure 5 Establishment of a reliable nomogram for predicting HCC prognosis. (**A** and **B**) Univariate and multivariate Cox regression models were utilized to uncover the association of clinical features and HRIG risk score with HCC survival outcome. (**C**) A prognostic nomogram was exploited by integrating independent prognostic indicators (pathological stage and risk score) to estimate 1-, 3-, and 5-year survival probability. (**D**) Calibration plots show the association of predicted 1-, 3-, and 5-year OS with actual survival duration. ***p < 0.001.

Discussion

Epidemiological studies have indicated a steady increase in the morbidity of HCC cases over time, which has been linked to various factors, such as hepatitis B virus infection, alcohol consumption, and genetic predisposition.[27–29] Despite advancements in diagnosing and treating HCC that have improved long-term outcomes and survival rates, the 5-year survival rate remains < 20%, which is unsatisfactory.[30–33] The lack of reliable diagnostic techniques for detecting early-stage HCC results has led to several patients being diagnosed only at advanced stages, thereby missing the window for potentially curative surgical interventions.[34–37] Therefore, it is crucial to discover new diagnostic biomarkers and therapeutic targets for early detection and improvement of patient prognosis.

Research indicates that HOXC9 is a vital transcription factor in embryonic development, impacting essential biological functions like cellular growth, differentiation, and apoptosis.[20,38] Multiple studies have highlighted abnormalities in the expression patterns of HOXC9 in different cancer types, demonstrating its dual role as an oncogene and a tumor suppressor.[39–48] Additionally, a significant relationship exists between the HOXC9 expression levels and the clinical and pathological characteristics of patients with cancer, suggesting its potential as a prognostic indicator in cancer treatment.

An analysis of TCGA database revealed that HOXC9 is upregulated in HCC tissues, leading to decreased OS in patients with HCC who exhibit elevated HOXC9 expression. Further research indicated that HOXC9 demonstrates a significant positive correlation with various immune cells. Through LASSO-Cox regression analysis, this study identified four genes—EGLN3, IMPDH1, LPCAT1, and MARCKSL1—and constructed an HRIG risk score model to stratify patients with HCC and predict their immune responses. The present research indicates that individuals classified

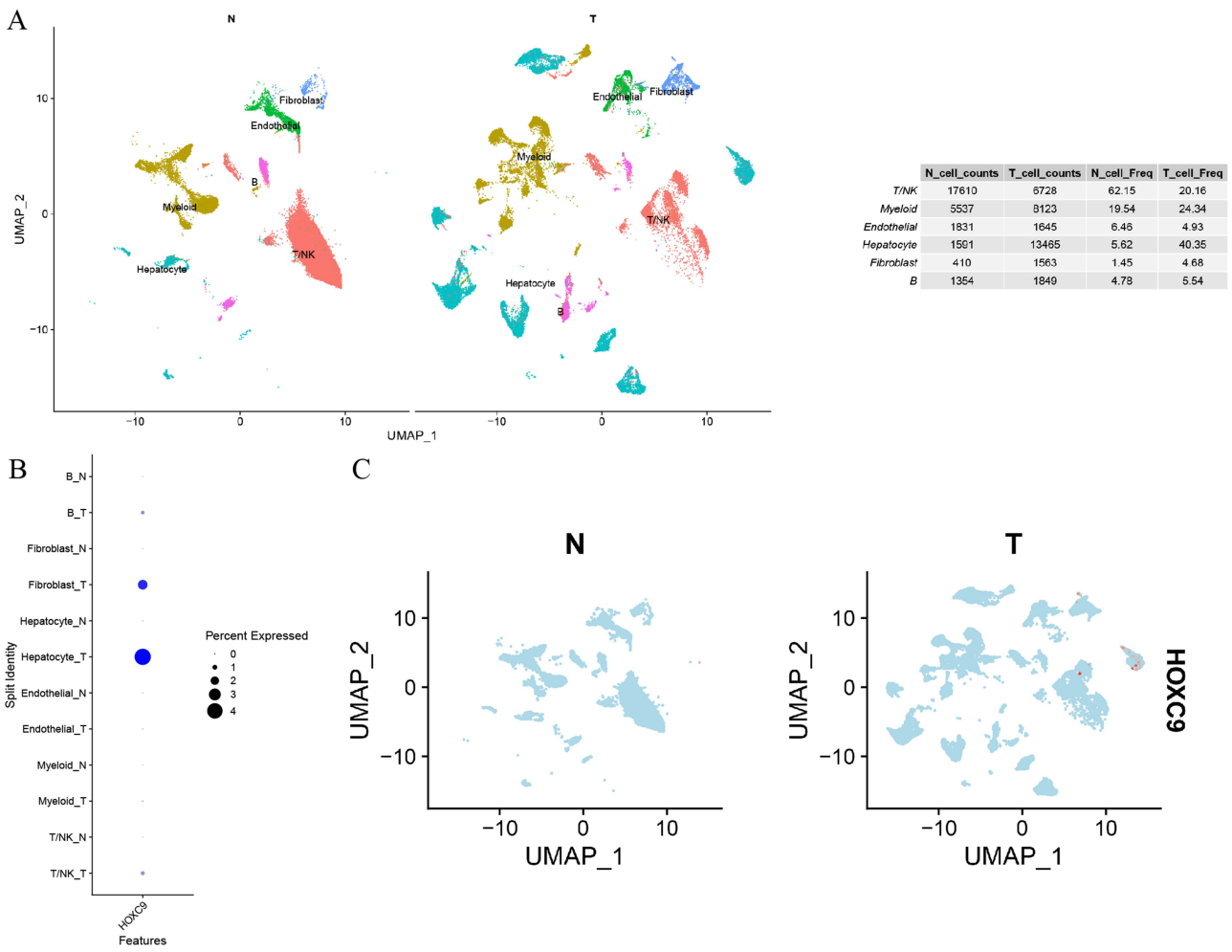

	N_cell_counts	T_cell_counts	N_cell_Freq	T_cell_Freq
T/NK	17610	6728	62.15	20.16
Myeloid	5537	8123	19.54	24.34
Endothelial	1831	1645	6.46	4.93
Hepatocyte	1591	13485	5.62	40.35
Fibroblast	410	1563	1.45	4.68
B	1354	1849	4.78	5.54

Figure 6 Cellular composition of the HCC tissue microenvironment. (**A**) Annotation of each cell type in HCC tissues and adjacent normal tissues. (**B**) Expression distribution of the HOXC9 gene in each cell type. (**C**) UMAP projections show the expression and distribution of HOXC9 in each cell type.

as high-risk have a decreased OS, and the nomogram accurately forecasted the survival rates at 1, 3, and 5 years for patients with HCC. In the GSE14520 cohort, the HRIG risk score model presented higher diagnostic efficacy, implying that the model has high clinical applicability. This study then evaluated the relationship between the model, TME, and immune cell infiltration. The findings indicate that individuals in the high-risk category exhibit elevated immune scores and increased immune cell infiltration. Hence, this study hypothesizes that immune cells play a crucial biological function in patients with high risk, potentially impacting the immune response.

Moreover, the study found that EGLN3, IMPDH1, LPCAT1, and MARCKSL1 play important roles in cancer biology and are closely related to immune responses and tumor progression. EGLN3 is a proline hydroxylase that affects tumor cell metabolism and hypoxic responses by regulating the HIF signaling pathway. Abnormal expression of EGLN3 is associated with increased tumor malignancy and may indirectly regulate immune cell function through the HIF signaling pathway.[49] IMPDH1 is a key enzyme in the synthesis of guanylate. Its overexpression in tumors promotes cell proliferation and survival, and its metabolic products may affect the activity of immune cells, thereby modulating the tumor microenvironment.[50] LPCAT1 is involved in phospholipid metabolism. Its overexpression in various cancers is associated with tumor proliferation, migration, and inhibition of apoptosis, and is closely related to immune cell infiltration and the expression of immune checkpoint genes, making it a potential predictive biomarker for immune therapy response.[51] MARCKSL1 regulates tumor cell migration and invasion by modulating cytoskeletal dynamics and

https://doi.org/10.2147/OTT.S509625

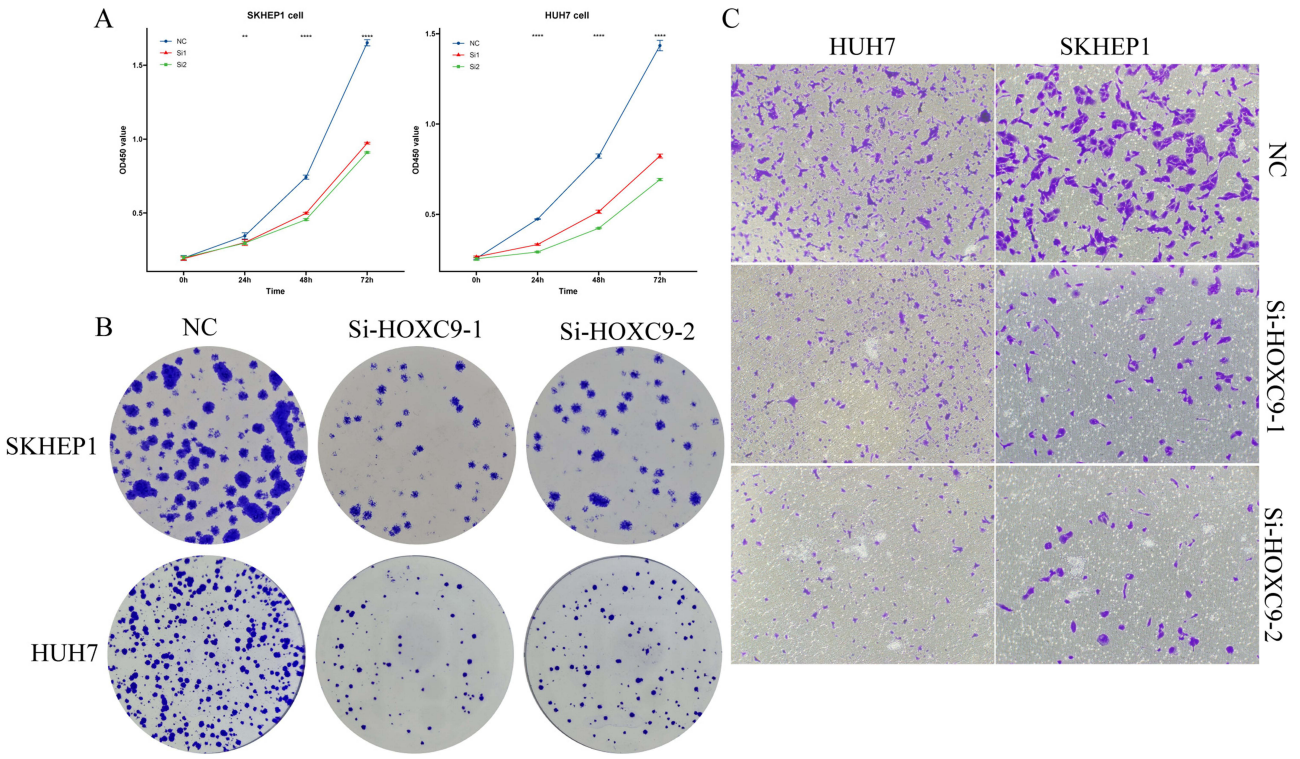

Figure 7 HOXC9 promotes HCC cell viability, colony formation, and invasion. (**A**) Cell viability of HUH7 cells or SKHEP1 cells that were transfected with control or si-HOXC9 was assessed using the CCK8 assay. (**B**) Colony formation assay was conducted to detect the proliferation of HUH7 cells and SKHEP1 cells. (**C**) Transwell assay was employed to examine cell invasion in control and HOXC9 knockdown cells. **p < 0.01, ****p < 0.0001.

may also affect the migration and function of immune cells through similar mechanisms, although its specific role in immune responses requires further investigation.[52] Overall, the complex roles of these genes in tumor progression and immune responses provide new perspectives and potential targets for the diagnosis and treatment of cancer.

In the IMvigor210 BLCA cohort, patients classified as high-risk showed a decreased immune response rate, whereas individuals in the SD/PD group had elevated risk scores. The group at high risk had more patients in advanced stages. KM curves demonstrated notable variations in survival rates among the high-risk and low-risk groups. Prior research indicates that individuals with tumors exhibiting increased immune cell infiltration are more inclined to respond positively to immunotherapy.[53] However, in the IMvigor210 cohort, patients with high risk exhibited lowered immune response. This could be due to the differences in tumor types, tumor heterogeneity, and smaller sample sizes. Hence, further investigation is required to clarify the potential molecular pathways. ScRNA-seq uncovered a notable augmentation in the levels of infiltrating hepatocytes and fibroblasts, alongside a reduction in the levels of T/NK cells in HCC tissue compared to adjacent normal tissues. Additionally, HOXC9 exhibited a significant upregulation in fibroblasts and hepatocytes within HCC tissues. These findings indicate that HCC tumorigenesis is linked to changes in immune cell infiltration levels and HOXC9 expression. In vitro experiments have confirmed that HOXC9 knockdown can significantly inhibit the viability, colony formation ability, and invasive capacity of HCC cells. Hence, HOXC9 functions as an oncogene and can be employed as an independent risk factor for individuals with HCC.

Although the current study provides valuable insights, there are still certain limitations. Firstly, the specific molecular mechanism by which HOXC9 promotes the malignant progression of HCC has not been fully understood, necessitating further research. Secondly, the association between HOXC9 and the TME requires further exploration.

However, although the current study provides valuable insights, there are still certain limitations. First, the specific molecular mechanism by which HOXC9 promotes the malignant progression of HCC still needs more in-depth study. Second, the association between HOXC9 and the TME still needs further exploration.

Conclusion

HOXC9 is overexpressed in HCC tissues and correlates with a reduced OS. This study constructed an HRIG risk score model using LASSO-Cox regression analysis for assessing the risk and predicting the immune response in patients with HCC. The results indicate that the high-risk group exhibits lowered immune responses and a higher proportion of patients in the advanced stage. In vitro experiments confirmed that HOXC9 downregulation can significantly inhibit the malignant phenotype of HCC cells.

Abbreviations

BLCA, bladder cancer; CR/PR, complete response/partial response; EMX, empty spiracles; FBS, fetal bovine serum; GEO, Gene Expression Omnibus; HCC, hepatocellular carcinoma; HOM-C, homeotic complex; HR, hazard ratio; HRIGs, HOXC9-related immune genes; ICIs, immune checkpoint inhibitors; irAEs, immune-related adverse events; KM, Kaplan-Meier; MSH, muscle segment homeobox; OTX, orthodenticle-related; OS, overall survival; PAX, paired-box; PBS, phosphate-buffered saline; PFS, progression-free survival; SD/PD, stable disease/progressive disease; si-HOXC9, small interfering-HOXC9; scRNA-seq, Single-cell RNA sequencing; TCGA, The Cancer Genome Atlas; TACE, transcatheter arterial chemoembolization; Treg, regulatory T; UMAP, uniform manifold approximation and projection.

Ethics Approval

This study complies with the Declaration of Helsinki. This study was approved by the ethical committee of the Lianyungang Municipal Oriental Hospital. Ethics Approval Number: 2024-041-01.

Author Contributions

All authors made a significant contribution to the work reported, whether that is in the conception, study design, execution, acquisition of data, analysis and interpretation, or in all these areas; took part in drafting, revising or critically reviewing the article; gave final approval of the version to be published; have agreed on the journal to which the article has been submitted; and agree to be accountable for all aspects of the work.

Funding

This work was supported by the Guidance Project of the Health Commission of Lianyungang City (grant no: ZD202206), and Research and Development Fund Project of Kanda College, Nanjing Medical University (grant no: KD2022KYJJZD137).

Disclosure

Yong Zhang and Hengliang Sun are co-first authors for this study. The authors have no relevant financial or non-financial interests to disclose for this work.

References

1. Chaudhry KA, Jacobi JJ, Gillard BM. et al. Aryl hydrocarbon receptor is a tumor promoter in MYCN-amplified neuroblastoma cells through suppression of differentiation. *iScience*. 2023;26(11):108303. doi:10.1016/j.isci.2023.108303
2. Pinter M, Jain RK, Duda DG. The Current Landscape of Immune Checkpoint Blockade in Hepatocellular Carcinoma: a Review. *JAMA Oncol*. 2021;7(1):113–123. doi:10.1001/jamaoncol.2020.3381
3. Liu Z, Liu X, Liang J, et al. Immunotherapy for Hepatocellular Carcinoma: current Status and Future Prospects. *Front Immunol*. 2021;12:765101. doi:10.3389/fimmu.2021.765101
4. Galle PR, Dufour J-F, Peck-Radosavljevic M, Trojan J, Vogel A. Systemic therapy of advanced hepatocellular carcinoma. *Future Oncol*. 2021;17 (10):1237–1251. doi:10.2217/fon-2020-0758
5. Wang Y, Deng B. Hepatocellular carcinoma: molecular mechanism, targeted therapy, and biomarkers. *Cancer Metastasis Rev*. 2023;42(3):629–652. doi:10.1007/s10555-023-10084-4
6. Sun H, Yang H, Mao Y. Personalized treatment for hepatocellular carcinoma in the era of targeted medicine and bioengineering. *Front Pharmacol*. 2023;14:1150151. doi:10.3389/fphar.2023.1150151
7. Laface C, Fedele P, Maselli FM, et al. Targeted Therapy for Hepatocellular Carcinoma: old and New Opportunities. *Cancers (Basel)*. 2022;14 (16):4028. doi:10.3390/cancers14164028

8. Liang H-Y, Liang Q-L, Chen M, Wang Z-W, Huang J. One case of comprehensive treatment for advanced liver cancer followed up over three years. *Arch Med Sci*. 2022;18(4):1112–1117. doi:10.5114/aoms/150440
9. Cong Z, Tran O, Nelson J, Silver M, Chung K. Productivity Loss and Indirect Costs for Patients Newly Diagnosed with Early- versus Late-Stage Cancer in the USA: a Large-Scale Observational Research Study. *Appl Health Econ Health Policy*. 2022;20(6):845–856. doi:10.1007/s40258-022-00753-w
10. Sahin TK, Rizzo A, Aksoy S, Guven DC. Prognostic Significance of the Royal Marsden Hospital (RMH) Score in Patients with Cancer: a Systematic Review and Meta-Analysis. *Cancers (Basel)*. 2024;16(10):1835. doi:10.3390/cancers16101835
11. Rizzo A, Ricci AD, Brandi G. Immune-based combinations for advanced hepatocellular carcinoma: shaping the direction of first-line therapy. *Future Oncol*. 2021;17(7):755–757. doi:10.2217/fon-2020-0986
12. Finn RS, Qin S, Ikeda M, et al. Atezolizumab plus Bevacizumab in Unresectable Hepatocellular Carcinoma. *N Engl J Med*. 2020;382(20):1894–1905. doi:10.1056/NEJMoa1915745
13. Kudo M. Atezolizumab plus Bevacizumab Followed by Curative Conversion (ABC Conversion) in Patients with Unresectable, TACE-Unsuitable Intermediate-Stage Hepatocellular Carcinoma. *Liver Cancer*. 2022;11(5):399–406. doi:10.1159/000526163
14. Zhao C, Xiang Z, Li M, et al. Transarterial Chemoembolization Combined with Atezolizumab Plus Bevacizumab or Lenvatinib for Unresectable Hepatocellular Carcinoma: a Propensity Score Matched Study. *J Hepatocell Carcinoma*. 2023;10:1195–1206. doi:10.2147/JHC.S418256
15. Rizzo A, Ricci AD, Brandi G. Trans-Arterial Chemoembolization Plus Systemic Treatments for Hepatocellular Carcinoma: an Update. *J Pers Med*. 2022;12(11):1788. doi:10.3390/jpm12111788
16. Rizzo A, Mollica V, Tateo V, et al. Hypertransaminasemia in cancer patients receiving immunotherapy and immune-based combinations: the MOUSEION-05 study. *Cancer Immunol Immunother*. 2023;72(6):1381–1394. doi:10.1007/s00262-023-03366-x
17. Rizzo A, Santoni M, Mollica V, et al. Peripheral neuropathy and headache in cancer patients treated with immunotherapy and immuno-oncology combinations: the MOUSEION-02 study. *Expert Opin Drug Metab Toxicol*. 2021;17(12):1455–1466. doi:10.1080/17425255.2021.2029405
18. Guven DC, Sahin TK, Erul E, et al. The association between albumin levels and survival in patients treated with immune checkpoint inhibitors: a systematic review and meta-analysis. *Front mol Biosci*. 2022;9:1039121. doi:10.3389/fmolb.2022.1039121
19. Stoll SJ, Bartsch S, Augustin HG, Kroll J. The transcription factor HOXC9 regulates endothelial cell quiescence and vascular morphogenesis in zebrafish via inhibition of interleukin 8. *Circ Res*. 2011;108(11):1367–1377. doi:10.1161/CIRCRESAHA.111.244095
20. Stoll SJ, Kroll J. HOXC9: a key regulator of endothelial cell quiescence and vascular morphogenesis. *Trends Cardiovasc Med*. 2012;22(1):7–11. doi:10.1016/j.tcm.2012.06.002
21. Svingen T, Tonissen KF. Hox transcription factors and their elusive mammalian gene targets. *Heredity*. 2006;97(2):88–96. doi:10.1038/sj.hdy.6800847
22. Duboule D. The vertebrate limb: a model system to study the Hox/HOM gene network during development and evolution. *Bioessays*. 1992;14(6):375–384. doi:10.1002/bies.950140606
23. Lu K, Wei S, Wang Z, et al. Identification of novel biomarkers in Hunner's interstitial cystitis using the CIBERSORT, an algorithm based on machine learning. *BMC Urol*. 2021;21(1):109. doi:10.1186/s12894-021-00875-8
24. Wang L, Yang Z, Cao Y. Regulatory T cell and activated natural killer cell infiltration in hepatocellular carcinoma: immune cell profiling using the CIBERSORT. *Ann Transl Med*. 2020;8(22):1483. doi:10.21037/atm-20-5830
25. Yoshihara K, Shahmoradgoli M, Martínez E, et al. Inferring tumour purity and stromal and immune cell admixture from expression data. *Nat Commun*. 2013;4:2612. doi:10.1038/ncomms3612
26. Petitprez F, Levy S, Sun C-M, et al. The murine Microenvironment Cell Population counter method to estimate abundance of tissue-infiltrating immune and stromal cell populations in murine samples using gene expression. *Genome Med*. 2020;12(1):86. doi:10.1186/s13073-020-00783-w
27. Yu MC, Yuan J-M, Lu SC. Alcohol, cofactors and the genetics of hepatocellular carcinoma. *J Gastroenterol Hepatol*. 2008;23(1):S92–S97. doi:10.1111/j.1440-1746.2007.05293.x
28. Wang H, Li W. Recent update on comprehensive therapy for advanced hepatocellular carcinoma. *World J Gastrointest Oncol*. 2021;13(8):845–855. doi:10.4251/wjgo.v13.i8.845
29. Zhang JY, M Dai, X Wang, et al. A case-control study of hepatitis B and C virus infection as risk factors for hepatocellular carcinoma in Henan, China. *Int J Epidemiol*. 1998;27(4):574–578. doi:10.1093/ije/27.4.574
30. McMahon B, Cohen C, Brown Jr RS, et al. Opportunities to address gaps in early detection and improve outcomes of liver cancer. *JNCI Cancer Spectr*. 2023;7(3). doi:10.1093/jncics/pkad034
31. Melendez-Torres J, Singal AG. Early detection of hepatocellular carcinoma: roadmap for improvement. *Expert Rev Anticancer Ther*. 2022;22(6):621–632. doi:10.1080/14737140.2022.2074404
32. Harris PS, Hansen RM, Gray ME, et al. Hepatocellular carcinoma surveillance: an evidence-based approach. *World J Gastroenterol*. 2019;25(13):1550–1559. doi:10.3748/wjg.v25.i13.1550
33. Song S, Bai M, Li X, et al. Early predictive value of circulating biomarkers for sorafenib in advanced hepatocellular carcinoma. *Expert Rev mol Diagn*. 2022;22(3):361–378. doi:10.1080/14737159.2022.2049248
34. He K, Yang Z, Liu X, et al. Identification of Potential Predictors of Prognosis and Sorafenib-Associated Survival Benefits in Patients with Hepatocellular Carcinoma after Transcatheter Arterial Chemoembolization. *Curr Oncol*. 2022;30(1):476–491. doi:10.3390/curroncol30010038
35. Liu W, R Wei, J Chen, et al. Prognosis prediction and risk stratification of transarterial chemoembolization or intraarterial chemotherapy for unresectable hepatocellular carcinoma based on machine learning. *Eur Radiol*. 2024;2024:1. doi:10.1007/s00330-024-10581-2
36. Stoll SJ, Bartsch S, Kroll J. HOXC9 regulates formation of parachordal lymphangioplasts and the thoracic duct in zebrafish via stabilin 2. *PLoS One*. 2013;8(3):e58311. doi:10.1371/journal.pone.0058311
37. Bi R, Wei W, Lu Y, et al. High hsa_circ_0020123 expression indicates poor progression to non-small cell lung cancer by regulating the miR-495/HOXC9 axis. *Aging*. 2020;12(17):17343–17352. doi:10.18632/aging.103722
38. Brune JE, Kern M, Kunath A, et al. Fat depot-specific expression of HOXC9 and HOXC10 may contribute to adverse fat distribution and related metabolic traits. *Obesity*. 2016;24(1):51–59. doi:10.1002/oby.21317
39. Cao Y-M, Wen D, Qu N, Zhu Y-X. Prognostic and clinical significance of HOXC9 and HOXD10 in papillary thyroid cancer. *Transl Cancer Res*. 2021;10(7):3317–3325. doi:10.21037/tcr-21-373

40. Hu M, Ou-Yang W, Jing D, Chen R. Clinical Prognostic Significance of HOXC9 Expression in Patients with Colorectal Cancer. *Clin Lab*. 2019;65. doi:10.7754/Clin.Lab.2019.190122.
41. Hur H, Lee J-Y, Yang S, et al. HOXC9 Induces Phenotypic Switching between Proliferation and Invasion in Breast Cancer Cells. *J Cancer*. 2016;7 (7):768–773. doi:10.7150/jca.13894
42. Lin Q, Geng J, Ma K, et al. RASSF1A, APC, ESR1, ABCB1 and HOXC9, but not p16INK4A, DAPK1, PTEN and MT1G genes were frequently methylated in the stage I non-small cell lung cancer in China. *J Cancer Res Clin Oncol*. 2009;135(12):1675–1684. doi:10.1007/s00432-009-0614-4
43. Lv L, Li Y, Deng H, et al. MiR-193a-3p promotes the multi-chemoresistance of bladder cancer by targeting the HOXC9 gene. *Cancer Lett*. 2015;357(1):105–113. doi:10.1016/j.canlet.2014.11.002
44. Tang Y, Wang T, Yu Y, Yan Y, Wu C. Upregulation of HOXC9 generates interferon-gamma resistance in gastric cancer by inhibiting the DAPK1/RIG1/STAT1 axis. *Cancer Sci*. 2021;112(9):3455–3468. doi:10.1111/cas.15043
45. Wang X, Choi J-H, Ding J, et al. HOXC9 directly regulates distinct sets of genes to coordinate diverse cellular processes during neuronal differentiation. *BMC Genomics*. 2013;14(1):830. doi:10.1186/1471-2164-14-830
46. Mao L, Ding J, Zha Y, et al. HOXC9 links cell-cycle exit and neuronal differentiation and is a prognostic marker in neuroblastoma. *Cancer Res*. 2011;71(12):4314–4324. doi:10.1158/0008-5472.CAN-11-0051
47. Turan T, Kongpachith S, Halliwill K, et al. iBRIDGE: a Data Integration Method to Identify Inflamed Tumors from Single-cell RNA-Seq Data and Differentiate Cell Type-Specific Markers of Immune-Cell Infiltration. *Cancer Immunol Res*. 2023;11(6):732–746. doi:10.1158/2326-6066.CIR-22-0283
48. Melssen MM, Sheybani ND, Leick KM, Slingluff CL. Barriers to immune cell infiltration in tumors. *J Immunother Cancer*. 2023;11:1. doi:10.1136/jitc-2022-006401
49. Cai F, Yang X, Ma G, et al. EGLN3 attenuates gastric cancer cell malignant characteristics by inhibiting JMJD8/NF-κB signalling activation independent of hydroxylase activity. *Br J Cancer*. 2024;130(4):597–612. doi:10.1038/s41416-023-02546-x
50. Zheng M-M, J Li, H Guo. et al. IMPDH inhibitors upregulate PD-L1 in cancer cells without impairing immune checkpoint inhibitor efficacy. *Acta Pharmacol. Sin.* 2024;2024:1. doi:10.1038/s41401-024-01411-8
51. Li Z, Hu Y, Zheng H, et al. LPCAT1-mediated membrane phospholipid remodelling promotes ferroptosis evasion and tumour growth. *Nat Cell Biol*. 2024;26(5):811–824. doi:10.1038/s41556-024-01405-y
52. Rong W, Shao S, Pu Y, Ji Q, Zhu H. Circulating extracellular vesicle-derived MARCKSL1 is a potential diagnostic non-invasive biomarker in metastatic colorectal cancer patients. *Sci Rep*. 2023;13(1):9957. doi:10.1038/s41598-023-37008-0
53. Chen F, Shen L, Wang Y, et al. Signatures of immune cell infiltration for predicting immune escape and immunotherapy in cervical cancer. *Aging*. 2023;15(5):1685–1698. doi:10.18632/aging.204583